Selective Patterning of Liquid Metal-Based Soft Electronics via Laser-Induced Graphene Residue

Wedyan Babatain
MIT Media Lab
Massachusetts Institute of Technology
Cambridge, MA, USA
wedyan@mit.edu

Ozgun Kilic Afsar
MIT Media Lab
Massachusetts Institute of Technology
Cambridge, MA, USA
ozgun@media.mit.edu

Fabian Velasquez
MIT EECS
Massachusetts Institute of Technology
Cambridge, MA, USA
fabianv@mit.edu

Hiroshi Ishii
MIT Media Lab
Massachusetts Institute of Technology
Cambridge, MA, USA
ishii@media.mit.edu

***Abstract*— Liquid metal-based flexible electronics hold promise for wearable devices that can monitor human activities unobtrusively. However, existing fabrication methods pose challenges in scalability and durability, especially for devices designed for daily use. In this study, we present a novel approach to pattern liquid metal using laser-induced graphene residue as a non-wetting barrier. The proposed method can resolve liquid metal traces up to 200 µm wide. The electrical and mechanical properties of the liquid metal traces enable these electronic devices to stretch up to 40% and bend with radii as small as 5mm, ensuring reliable connectivity for wearable human-machine interfaces. Furthermore, by transferring optimized liquid metal patterns onto a PDMS substrate, we successfully demonstrate a range of soft electronic devices that enable accessible and conformal interface with the human body without mechanical limitations.**

Keywords— Liquid Metal, Liquid Metal Patterning, Flexible electronics, wearables, Laser-induced graphene

I. INTRODUCTION

Liquid Metal (LM) electronics offer great potential for body sensor networks due to their fluidic characteristics such as conformability and stretchability, while having the ability to self-heal and maintain their conductive properties. LM has been extensively leveraged in many soft electronics applications from wearables and soft robots to smart textiles and self-healing reconfigurable electronics [1] . One advantage of LM is its ability to maintain functionality under mechanical stress, making it a robust candidate for flexible application. Body sensor networks benefit from LM's mechanical robustness with the possibility of higher fidelity sensing compared to conventional inflexible devices[2]. Examples of wearable LM devices include capacitive tactile sensors, strain sensing, and pulse sensing [1], [3], [4]. However, fabricating functional LM circuits and devices present challenges due to its fluidic nature and its oxide layer. Numerous patterning methods exist, each with its own advantages and limitations. Patterning affects resolution, conductivity, and how much of LM's flexibility can be utilized. For example, injecting LM into patterned channels constrains the resulting device's conformability by the substrate and the channels that collapse if soft or wide[1]. Patterning methods can also be involved with complex instruments that prevent accessibility to LM electronics fabrication. Other patterning methods include direct ink writing (DIW) roller-ball pens and stencil printing with aerosols[2],[5]. Serial additive or subtractive approaches such as DIW, suffer from low throughput[2]. Parallel fabrication methods, such as stencil printing and transfer printing, face cost and stability issues associated with changing stencils or stamps due to the presence of the oxide layer[2]. Molds and microfluidics-based approaches are limited by low resolution and the need for specific channel characteristics to accommodate LM's high surface tension. yielding low resolution[2].While various patterning methods exist, each has its drawbacks, including substrate constraints, process speed, and resolution. This paper proposes a patterning method that can address some of these drawbacks while significantly increasing accessibility.

II. MATERIALS AND METHODS

A. Overview

In this study, we exploit the unique properties of laser-induced graphene (LIG), a graphene-based material formed through laser irradiation of commercial polyamide substrates to achieve selective patterning of LM electronics[6]. LIG has been shown to exhibit high non-wetting characteristics when in contact with LM, owing to its distinct surface properties[7]. The interconnected graphene flakes within LIG form a three-dimensional porous structure with a high aspect ratio, resulting in a rough and non-wetting surface to liquid metal. This roughness and non-wettability serve as deterrents, preventing the adhesion and spreading of LM on the treated regions. The non-wetting behavior of LIG can be attributed to the surface roughness introduced by the porous structure of LIG that leads to microscale and nanoscale irregularities on the substrate surface[8]. These irregularities increase the contact area between LIG and LM, consequently enhancing the surface tension forces that resist wetting. The presence of gaps and irregularities within the LIG structure hinders the intimate contact and spreading of the LM across the laser-graphitized areas. The chemical interactions between LIG and the LM promotes non-wetting properties as LM forms droplets or beads rather than spreads when it interacts with LIG directly [8]. This property has been effectively utilized in the development of LM sensors, where a direct interface with LIG necessitates the non-wetting and non-stick properties[9]–[11]. By exploiting these characteristics, LIG can act as an effective barrier during the patterning process, selectively confining LM to specific regions. This capability enables precise and controlled deposition of LM for the fabrication of complex electronic circuits and devices. The desired regions of the substrate are coated with LIG residue, and subsequently, LM is applied. LIG acts as a barrier, preventing the LM from wetting the treated areas. This non-wetting behavior enables precise patterning of LM circuits with high resolution and good reproducibility. The incorporation of LIG residue in the desired regions of the substrate, combined with the selective application of LM, allows for the realization of well-defined and accurately patterned LM circuits.

B. Fabrication Process

Our proposed facile fabrication method is illustrated in Figure 1. The process starts with the selective irradiation of a commercially available polyamide sheet using a CO2 laser with optimized power and speed. A negative mask, acting as a dark field mask, of the desired pattern is created from LIG. Subsequently, any excess LIG flakes are meticulously removed manually using a paper cloth to prevent unwanted flakes from being transferred during subsequent steps, leaving a residual gray layer of LIG just enough to act as a barrier. Next, eutectic gallium-indium (EGaIn) LM is carefully brushed onto the as-patterned LIG substrate.The non-wetting and LM-phobic properties of LIG prevent the LM from adhering to the laser-scribed areas, ensuring that the LM pattern forms exclusively on the untreated regions of polyamide.

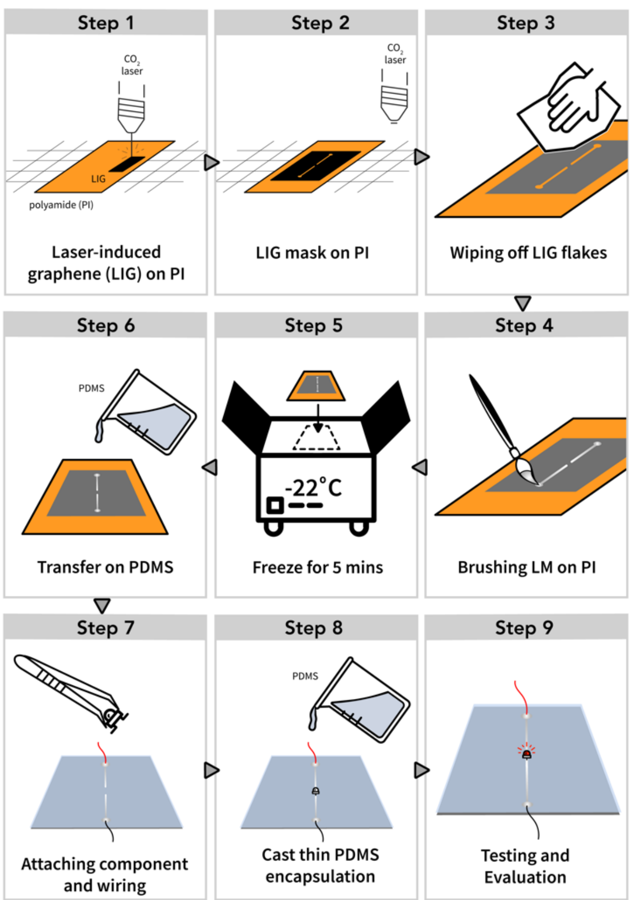

Fig. 1. Schematic illustration of the fabrication process flow of the proposed liquid metal patterning method.

To facilitate the subsequent casting of polydimethylsiloxane (PDMS) on the patterned substrate, the sample is placed in a freezer at -22°C for 5 minutes. Following the cooling step, PDMS is casted on top of the patterned substrate. The casted substrate is then allowed to cure at 60°C for 2 hours in an oven.Once the PDMS has completely cured, it is gently released from the polyimide substrate, allowing only the LM pattern to be transferred onto the PDMS surface. Finally, the desired electronic components are assembled onto the LM trace, and a thin layer of PDMS is casted on top as an encapsulation layer, securely affixing all components in place. This methodology enables the creation of precise and selective LM patterns on flexible substrates, providing a versatile platform for the integration of electronic components.

III. Results and Discussion

A. Physical Characterization of Patterned LM Traces

Figure 2 shows microscopic images of LM lines fabricated using the proposed method and showcasing the optical characterization. The LIG-assisted patterning method demonstrates excellent resolution, reaching up to 200 µm. As depicted in the figure, the patterned LM lines widths were 200, 300 and 400 µm on polyamide substrate prior to transfer. The images clearly illustrate the continuity of the LM lines and the distinct boundary between the lines and the laser-irradiated polyamide regions. Furthermore, Figure 2 also displays the same LM lines after their successful transfer into PDMS using the previously described casting method. The transferred lines maintain their integrity and continuity, highlighting the reliability and effectiveness of the transfer step.

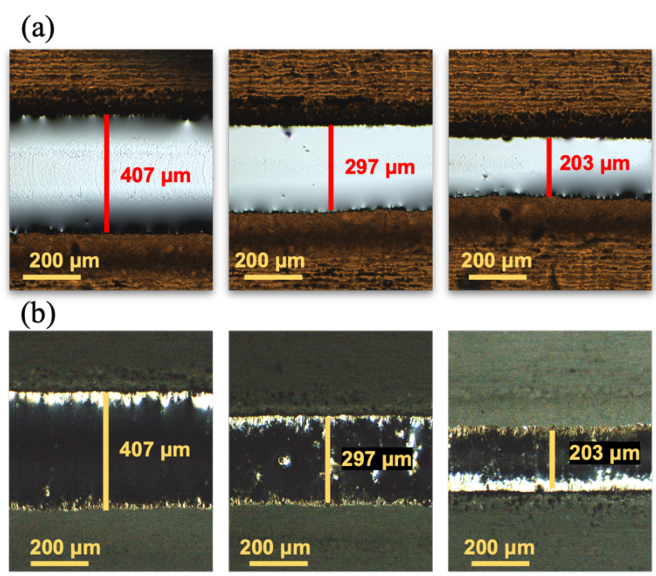

Fig. 2. Microscopic images of (a) the brushed LM traces with different widths on polyamide substrate and (b) the same traces after its transfer on PDMS substrate.

Figure 3a presents microscopic images highlighting the dewetting behavior of laser-graphitized areas to LM, showing its selective adherence to untreated polyamide regions. This results in distinct conductive patterns, of recognizable features such as by MIT logo. Figures 3b depict LM patterns post-transfer onto a flexible PDMS substrate, maintaining pattern integrity. The technique enables diverse designs like letters, logos, and complex patterns, demonstrating its versatility and potential for various conductive LM patterns on flexible substrates."

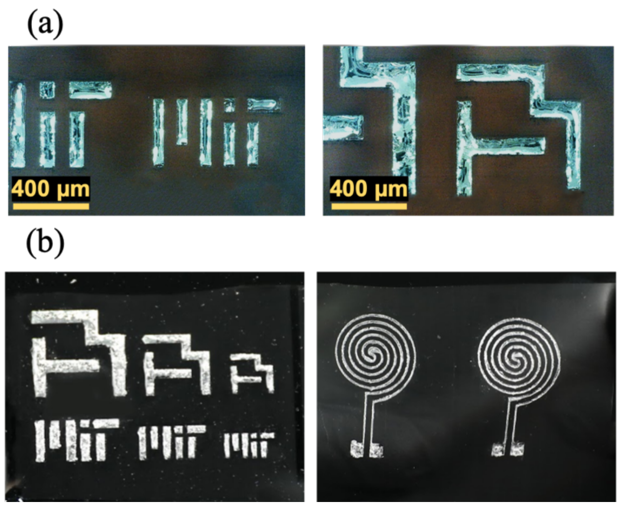

Fig. 3. (a) Microscopic images of patterned fabricated by the proposed method. (b) Optical images of liquid metal patterns after transfer to PDMS.

B. Mechanical and Electrical Characterization

Photographs depicting a fabricated 30x300 µm LM electrode that is in its initial state, as well as under stretching, twisting, and bending conditions, are shown in Figure 4.

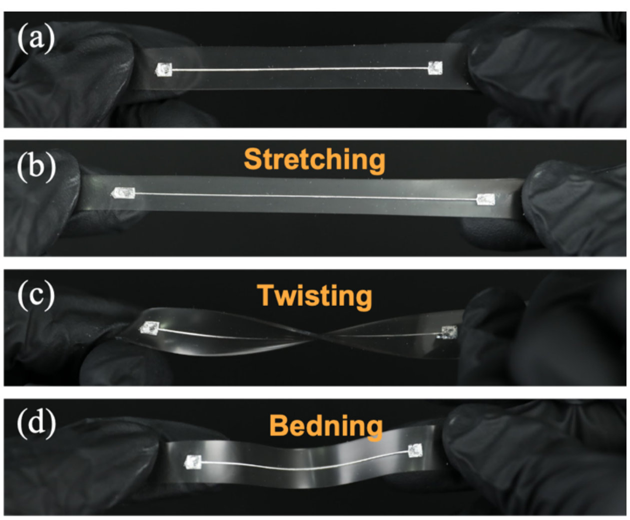

Fig. 4. (a) 300 µm thick LM trace maintaining its integrity after the transfer process on PDMS: (a) relaxed state, (b) stretched, (c) twisted and (d) bent.

To assess its potential for flexible and stretchable on-body electronics, the electrical resistance of the electrode was measured under various mechanical deformations. A custom-built motorized linear stage was employed for the mechanical-electrical characterization. Figure 5a shows the relative resistance change (ΔR/R0) of the LM electrode over time when subjected to 6 bending cycles for different bending radii including 15, 12.5, 10, and 7.5 and 5 mm.

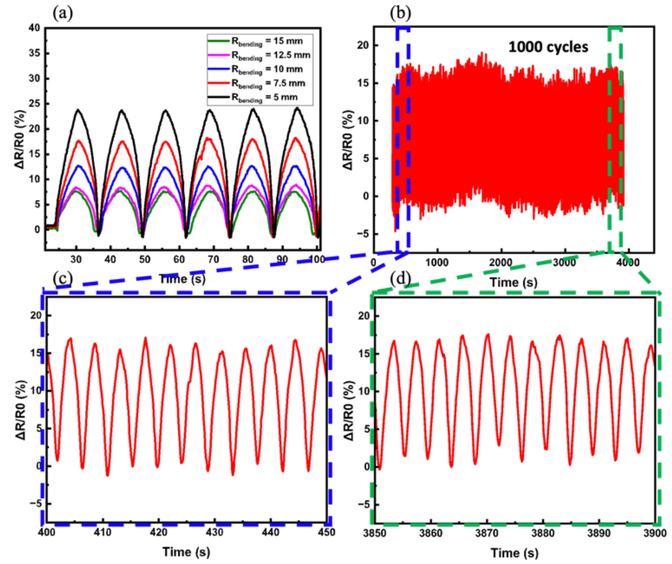

Fig. 5. Electrical performance of bending tests of LM trace. a) Relative change in resistance as a function of different bending radii (from 5 mm to 15mm). b) cycling bending test of a total of 1000 cycles with a bending radius of 7.5 mm.

The rise in resistance of the electrode is of a repeatable pattern, serving as a proof of the stability of the LM patterned electrode.

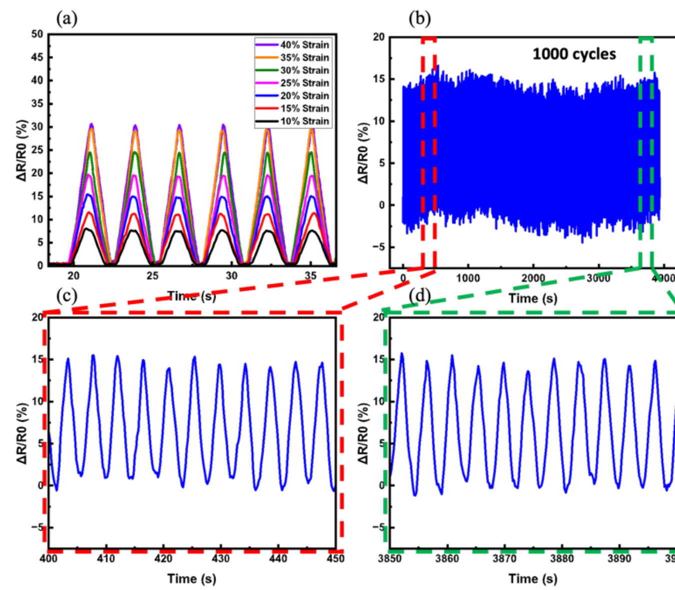

Fig. 6. Electrical performance of strain test Of LM trace. a) Relative change in resistance as a function of strain (from 10% to 40%) for LM trace transferred to a PDMS substrate. b) cyclic strain test of a total of 1000 cycles at 20% strain.

A bending cyclic test of 1000 cycles at radius of 7.5mm is shown in figure 5b. Zoomed in graphs show that the electrode exhibits resistance change and signals repeatability without any hysteresis .Moreover, the LM-patterned substrate was subjected to different linear strain percentages ranging from 10 to 40% as depicted in figure 6a. The result of the cyclic stretching test at 20% stain is shown in figure 6b. Throughout the 1000 cycles of repeated strain, the LM electrode exhibited excellent stability. These experiments confirm a stable electrical performance, even for an applied bending radius of 7.5 mm, or a strain of 40% for a long period of time.

IV. Device Integration

To demonstrate the utility of our developed method, we developed various devices including an LED circuit, a resistive pressure sensor and a capacitive touch sensor. Figure. 7a shows the LED-Integrated LM circuit before and after stretching. The LM wire maintained its continuity during the stretched state indicated by the illuminated LED, suggesting that the stress-induced resistance variation in the wires is negligible. Figure 7b shows the performance of resistive LM pressure sensor employing a spiral design. Upon applying pressure using a finger, the cross-sectional area of the LM electrode decreases, leading to an increase in its resistance. The results demonstrate the relative change in resistance ($\Delta R/R0$) of the resistive sensor in response to a sequence of finger presses, gradually increasing in pressure. This confirms the proportional relationship between the stress applied and the electrode resistance. Finally, we developed a capacitive touch sensing array consisting of multiple LM pads. The touch sensor consists of a square-shaped LM acting as a capacitive plate, which is encapsulated with a thin layer of PDMS to form the dielectric coating. When a finger touches the plate, the charge distribution alters the electric field, resulting in a corresponding increase in capacitance. The sensor can detect touch and untouched states. Figure 7c depicts the relative change in capacitance, demonstrating the variations in capacitance of the touch sensor pad between the untouched and touched states over two repeated cycles.

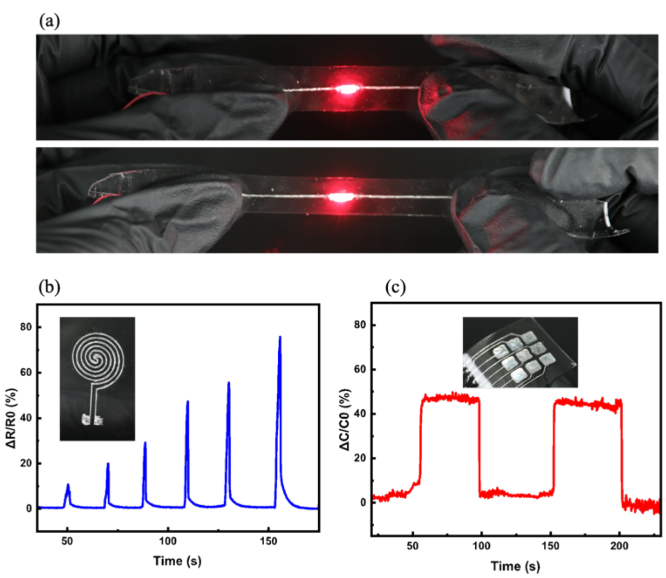

Fig. 7. a) LED-integrated liquid metal circuit. b) Relative change in resistance of the resistive pressure sensor upon gradual increase of finger press. c) Relative change in capacitance of the capacitive sensor upon when alternating intervals of finger touch is applied.

V. Conclusion and Outlook

In summary, we presented a facile method leveraging LIG to selectively pattern LM electronics. The proposed process enables the deposition of LM onto desired regions while preventing its adhesion to the LIG-treated areas. The method can produce patterns with excellent resolution. The ability to integrate LM electronics seamlessly into wearable devices opens new avenues for the development of advanced and functional conformable body-worn sensors. The integration of various electronic components, such as LED circuits, pressure sensors, and touch sensors, further illustrates the versatility of the method. Current sources of improvement includes precise and repeatable control of the thickness of the LM patterned traces and improving the quality of the transferred pattern. Additionally, investigations into the long-term stability of the fabricated devices under various environmental conditions would be crucial for their practical implementation. With further refinements, this method has the potential to reshape the landscape of electronic systems for healthcare and human-machine interfaces. Exploring the integration of additional electronic functionalities, such as wireless communication and energy harvesting, would further enhance the potential applications of LM based electronics.

Acknowledgment

The authors gratefully acknowledge funding from the KACST-MIT Ibn Khaldun Fellowship to W.B.

References

[1] J. Ma, F. Krisnadi, M. H. Vong, M. Kong, O. M. Awartani, and M. D. Dickey, “Shaping A Soft Future: Patterning Liquid Metals,” *Adv. Mater.*, p. 2205196, Aug. 2022, doi: 10.1002/adma.202205196.

[2] M. Kim, H. Lim, and S. H. Ko, “Liquid Metal Patterning and Unique Properties for Next-Generation Soft Electronics,” *Adv. Sci.*, vol. 10, no. 6, p. 2205795, Feb. 2023, doi: 10.1002/advs.202205795.

[3] C. B. Cooper *et al.*, “Stretchable Capacitive Sensors of Torsion, Strain, and Touch Using Double Helix Liquid Metal Fibers,” *Adv. Funct. Mater.*, vol. 27, no. 20, p. 1605630, May 2017, doi: 10.1002/adfm.201605630.

[4] S. Veerapandian *et al.*, “Hydrogen-doped viscoplastic liquid metal microparticles for stretchable printed metal lines,” *Nat. Mater.*, vol. 20, no. 4, pp. 533–540, Apr. 2021, doi: 10.1038/s41563-020-00863-7.

[5] T. V. Neumann and M. D. Dickey, “Liquid Metal Direct Write and 3D Printing: A Review,” *Adv. Mater. Technol.*, vol. 5, no. 9, p. 2000070, Sep. 2020, doi: 10.1002/admt.202000070.

[6] J. Lin *et al.*, “Laser-induced porous graphene films from commercial polymers,” *Nat. Commun.*, vol. 5, no. 1, p. 5714, Dec. 2014, doi: 10.1038/ncomms6714.

[7] Y. Chen *et al.*, “Robust Fabrication of Nonstick, Noncorrosive, Conductive Graphene-Coated Liquid Metal Droplets for Droplet-Based, Floating Electrodes,” *Adv. Funct. Mater.*, vol. 28, no. 8, p. 1706277, 2018, doi: 10.1002/adfm.201706277.

[8] J. Nasser, J. Lin, L. Zhang, and H. A. Sodano, “Laser induced graphene printing of spatially controlled super-hydrophobic/hydrophilic surfaces,” *Carbon*, vol. 162, pp. 570–578, Jun. 2020, doi: 10.1016/j.carbon.2020.03.002.

[9] W. Babatain, N. El-atab, and M. M. Hussain, “Graphene Coated Liquid Metal Droplet-Enabled Dual-Axis Integrated Accelerometer,” *Adv. Mater. Technol.*, vol. 8, no. 1, p. 2201094, 2023, doi: 10.1002/admt.202201094.

[10] W. Babatain, U. Buttner, N. El-Atab, and M. M. Hussain, “Graphene and Liquid Metal Integrated Multifunctional Wearable Platform for Monitoring Motion and Human–Machine Interfacing,” *ACS Nano*, vol. 16, no. 12, pp. 20305–20317, Dec. 2022, doi: 10.1021/acsnano.2c06180.

[11] K. Xu *et al.*, “A Wearable Body Condition Sensor System with Wireless Feedback Alarm Functions,” *Adv. Mater.*, vol. 33, no. 18, p. 2008701, May 2021, doi: 10.1002/adma.202008701.